Mechanistic Model of Slug Flow in Near-Horizontal Pipes

P. Andreussi, A. Minervini, and A. Paglianti
Dept. of Chemical Engineering and Materials Science, University of Pisa, Pisa, Italy

A mechanistic model of slug flow based on a set of mass and momentum conservation equations and a number of empirical closure relations is presented. It is then shown that a simplified version of the model, which physically corresponds to the flow of long liquid slugs (long slug model, LSM), can be immediately derived from the general model. The LSM is much simpler than the general model; at the same time, the predictions obtained in the two cases are very similar, when the comparison is limited to the computation of the pressure gradient and the mean liquid holdup. The LSM successfully correlates a large set of experimental measurements relative to three pipe diameters (18, 50 and 90 mm), four inclinations (0°, ±3°, 0.3°), and two pipe lengths (17 and 34 m).

Introduction

In pipe flow of gas-liquid mixtures, slug or intermittent flow conditions are encountered for a wide range of gas and liquid superficial velocities. This flow pattern can be described as a stratified flow with the intermittent appearance of aerated liquid slugs traveling at high velocity. At increasing liquid rates, the slug frequency increases and the transition to dispersed bubble flow is approached. This flow pattern is characterized by a continuous liquid phase in which small gas bubbles of spherical shape are dispersed. At low liquid flows, the slugs are not able to bridge the whole pipe cross section and the stable flow patterns will be stratified wavy or annular flow. In the range of low gas velocities, the elongated bubble, or the plug-flow regime is encountered. It is usually assumed that the main difference between elongated bubble and slug flow is that in slug-flow dispersed gas bubbles are entrained into the slugs. As discussed by Ruder and Hanratty (1989), the distinction between slug and elongated bubble flow can also be based on different structural characteristics of these flow patterns.

In practical applications, such as the prediction of the pressure gradient and the liquid holdup in pipelines transporting gas-liquid mixtures, it may be convenient to use a unique predictive model for the slug and elongated bubble or plug-flow patterns. Moreover, as slug flow can be considered as a combination of dispersed bubble and stratified flow, slug-flow models should contain, as particular cases, the description of these flow patterns.

A mechanistic model of intermittent flow has been developed by Dukler and Hubbard (1975), and tested with data taken in small diameter, horizontal pipes. Nicholson et al. (1978) modified this model, without introducing substantial changes in the original set of equations proposed by Dukler and Hubbard. The main assumption made by Dukler and Hubbard has been that slug flow can be represented by a sequence of identical slug units traveling at a constant translational velocity. This picture has been confirmed by an extensive statistical analysis of main slug parameters recently presented by Nydal et al. (1992). Fabre et al. (1983) proposed a more general multicell model of slug flow, in which the length of the slug unit is assumed to have a stochastic distribution. In order to solve model equations in this case it is necessary to introduce a number of simplifying assumptions, which finally lead to a model similar to the previous ones.

Although available slug-flow models successfully describe the experimental measurements, empirical correlations, with no reference to a specific flow regime, are still preferred in the design of gas-liquid pipelines. Reasons for this choice appear to be:

- The structure of available models of slug flow is rather complex.
- Closure relations of empirical or semi-empirical origin are needed to predict void in the slugs, slug velocity and, eventually, other flow parameters.
- The boundaries of the slug-flow regime, and hence the region of applicability of the model, are uncertain.

In this article, a fairly general, one-dimensional slug-flow model is presented. It is then shown that a simplified version of this

model, which physically corresponds to the flow of long liquid slugs (long slug model, LSM), immediately arises from the general model. The LSM is finally compared with a large set of data relative to three pipe diameters, four inclinations and a wide range of gas and liquid flow rates, which cover the slug, the elongated, and the dispersed bubble flow patterns.

Analysis

Physical model

A schematic diagram of the flow model is shown in Figure 1. The model proposed by Dukler and Hubbard is based on the main assumptions:

- slug flow is represented by a sequence of identical slug units traveling at a constant translational velocity.
- The slip between gas and liquid in the slug body is neglected.
- The liquid film following the slug does not contain dispersed bubbles.

In the present model, gas expansion along the pipe is accounted for. This somewhat modifies the first assumption, as the slug velocity depends on the local value of the gas density. An estimate of the effects of slip in the slug body and of film aeration indicates that they should not be significant. This allows to assume for the model a structure similar to that proposed by Dukler and Hubbard, the main difference being in the closure equations adopted in the two cases. Besides this, the equations describing the stratified flow region are more general and complete.

The flow model is based on the mass conservation equations for the liquid and the gas phases,

$$j_l=\frac{1}{l_u}\int_o^{l_f} v_f H_f dx + H_s v_s \frac{l_s}{l_u}, \tag{1}$$

$$j_g=\frac{1}{l_u}\int_o^{l_f} v_b(1-H_f)dx + (1-H_s)v_s\frac{l_s}{l_u}. \tag{2}$$

In Eq. 2, j_g is the superficial gas velocity, obtained from the known value of the gas flow rate and from the local value of the gas density, v_s is the mean velocity of the liquid and the gas in the slug body, v_f and v_b are the mean velocities of the liquid and the gas in the stratified flow region. As the height of the liquid layer, or the liquid holdup, H_f, varies along the axial coordinate, v_f and v_b are functions of x.

Continuity equations relative to an observer traveling at the translational velocity of the slug unit, v_t, can be written as

$$(v_t-v_f)H_f=(v_t-v_s)H_s, \tag{3}$$

$$(v_t-v_b)(1-H_f)=(v_t-v_s)(1-H_s). \tag{4}$$

The translational slug velocity is usually expressed as (see Nicklin et al., 1962, Dukler and Hubbard, Nicholson et al., and Bendiksen, 1984)

$$v_t=c_o v_s+v_o. \tag{5}$$

In Eq. 5, v_o becomes negligible and $c_o\simeq 1.2$ for large values of the mixture velocity or, as suggested by Bendiksen (1984), when the bubble nose becomes centered.

The liquid holdup in the slugs can be obtained from the semi-empirical correlation recently proposed by Andreussi and Bendiksen (1989)

$$H_s=1-\frac{Fr_m-F_o}{Fr_m+F_1}, \tag{6}$$

where Fr_m is a Froude number based on the mixture velocity, $v_m=j_g+j_l$,

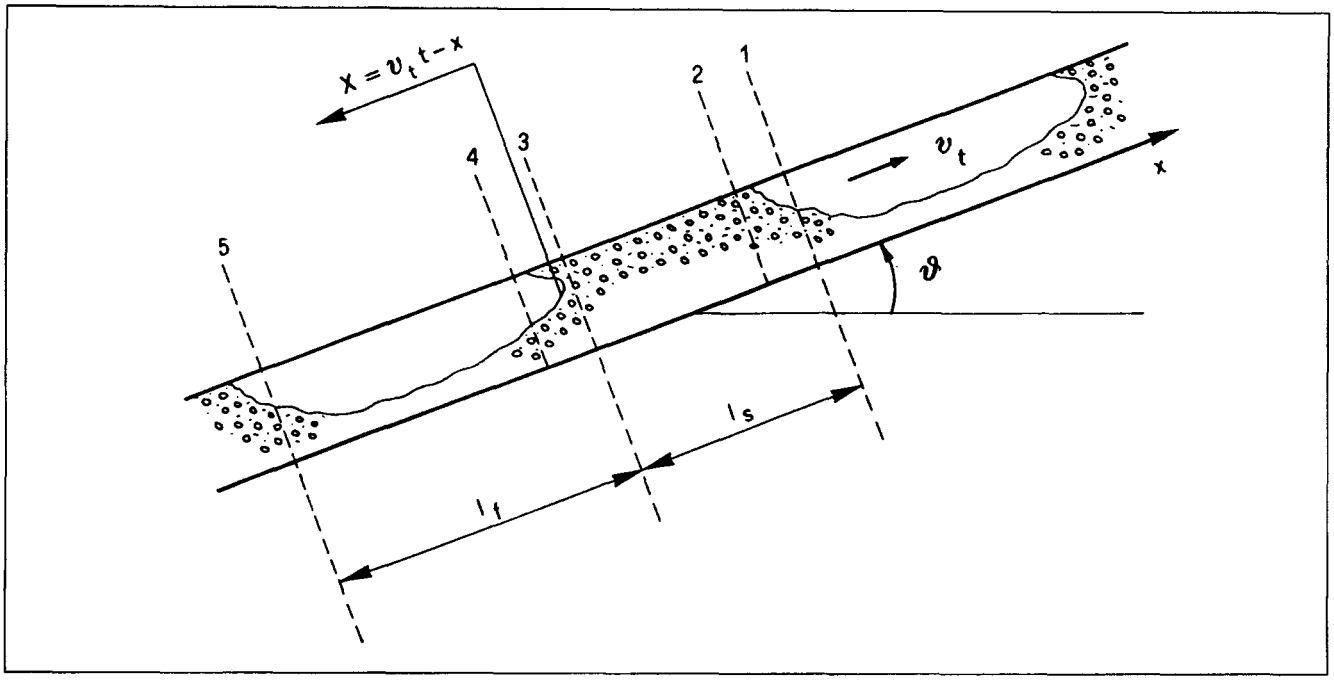

Figure 1. Flow model.

$$Fr_m = \frac{v_m}{\sqrt{gD}}. \tag{7}$$

In Eq. 6, the parameters F_o and F_1 depend on pipe diameter and physical properties. The complete set of equations used for v_t and H_s is reported in the Appendix.

Equations 3 and 4 can be used to replace the products $v_f H_f$, $v_b(1-H_f)$ in Eqs. 1 and 2 with simpler expressions. Defining the mean film holdup as

$$\overline{H}_f = \frac{1}{l_f}\int_o^{l_f} H_f dx, \tag{8}$$

it is obtained

$$j_l = H_s v_s - (H_s - \overline{H}_f)\frac{l_f}{l_u} v_t, \tag{9}$$

$$j_g = (1-H_s)v_s + (H_s - \overline{H}_f)\frac{l_f}{l_u} v_t. \tag{10}$$

Equations 9 and 10 give

$$v_m = j_l + j_g = v_s. \tag{11}$$

The mean liquid holdup in the slug unit, H_l, defined as

$$H_l = \frac{H_s l_s + \overline{H}_f l_f}{l_u}, \tag{12}$$

can be computed from Eqs. 9 and 11 as

$$H_l = \frac{j_l + H_s(v_t - v_m)}{v_t}. \tag{13}$$

According to Eq. 13, H_l is entirely independent from the shape of the slug tail. This analytical result has not been reported by Dukler and Hubbard or Nicholson et al.

The pressure gradient is given by the sum of the frictional, gravitational and acceleration terms

$$-\frac{dP}{dx} = -\left(\frac{dP}{dx}\right)_F - \left(\frac{dP}{dx}\right)_G - \left(\frac{dP}{dx}\right)_A. \tag{14}$$

The acceleration term is only related to gas expansion effects and can be expressed as

$$-\left(\frac{dP}{dx}\right)_A = \rho_l j_l \frac{dv_l}{dx} + \rho_g j_g \frac{dv_g}{dx}. \tag{15}$$

The mean liquid and gas velocities, v_l and v_g, are given by

$$v_l = \frac{j_l}{H_l}, \quad v_g = \frac{j_g}{1-H_l}. \tag{16}$$

When the gas and the liquid mass flow rates are constant, Eq. 15 becomes

$$-\left(\frac{dP}{dx}\right)_A = -\left(\frac{\rho_l j_l^2}{H_l^2} - \frac{\rho_g j_g^2}{(1-H_l)^2}\right)\frac{dH_l}{dx} - \frac{j_g^2}{(1-H_l)}\frac{d\rho_g}{dx}. \tag{17}$$

The derivatives in the righthand side of Eq. 17 can be computed using Eq. 13 for H_l and the equation of state for ρ_g, assuming that the flow is isothermal.

The frictional and gravitational terms can be obtained from the equation

$$-\left(\frac{dP}{dx}\right)_F - \left(\frac{dP}{dx}\right)_G = \frac{\Delta P_u}{l_u} \tag{18}$$

where ΔP_u is the pressure drop through a slug unit, computed under the assumption of incompressible flow. ΔP_u can be derived from the momentum balances relative to the various positions along the slug unit indicated in Figure 1.

The pressure drop at the slug front, ΔP_{21}, is given by:

$$\Delta P_{21} = \rho_l g \cos\theta\left(\xi_1 - \frac{D}{2}H_s\right) + \rho_l H_s(v_t - v_s)[v_s - v_f(l_f)], \tag{19}$$

where ξ_1 is the depth of the center of pressure and $v_f(l_f)$ is the mean velocity in the liquid film at position 1 ($X = l_f$). The second term in the RHS of Eq. 19 can be seen as a recoverable pressure drop due to the acceleration of the liquid layer entrained at the slug front to the slug velocity. For simplicity, in Eq. 19 the hydrostatic head and the acceleration term relative to the gas entrained in the advancing slug have been neglected.

The pressure drop relative to the slug body, ΔP_{32}, can be related to frictional losses at pipe wall and to gravitational losses,

$$\Delta P_{32} = \left(\frac{4}{D}\tau_{ws} + \rho_m g \sin\theta\right) l_s, \tag{20}$$

where ρ_m is the mixture density, defined as:

$$\rho_m = H_s\rho_l + (1-H_s)\rho_g. \tag{21}$$

Dukler and Hubbard and Nicholson et al. assumed that the gas and the liquid in the slug form a homogeneous mixture, with mean density given by Eq. 21. They then computed the frictional pressure gradient by the same procedure usually adopted in single-phase pipe flow.

Present measurements cover also the bubble flow pattern and indicate that measured pressure gradients can be much larger (up to 30%) than the values computed using the homogeneous flow approximation. A much better agreement with measurements is obtained expressing the wall shear stress in dispersed bubble flow, τ_{wd}, as:

$$\tau_{wd} = \phi_d \tau_{wl}, \tag{22}$$

where τ_{wl} is the wall shear stress relative to the liquid phase flowing alone in the pipe and the coefficient ϕ_d can be expressed by the empirical correlation proposed by Malnes (1983), which is similar in its structure to the equation developed for vertical bubbly flow by Marie (1987). In these equations, ϕ_d depends on the liquid holdup and on the ratio between the rise velocity of a bubble and the mixture velocity,

$$\phi_d = f(H_s, v_\infty/v_m). \tag{23}$$

Eq. 23 is given in the Appendix.

The pressure drop at the nose of the elongated gas bubble, ΔP_{43}, is given by the momentum balance

$$\Delta P_{43}=\rho_l g\cos\theta\left(H_s\frac{D}{2}-\xi_4\right)-\rho_l H_s(v_t-v_s)[v_s-v_f(0)]. \quad (24)$$

As reported by Bendiksen (1984), in slug flow, for values of the mixture Froude number larger than 3.5, the nose of the elongated gas bubble moves from the top to the center of the pipe. Under these conditions, it seems reasonable to assume $H_f(0)\simeq H_s$, $v_f(0)\simeq v_s$, and $\Delta P_{43}\simeq 0$, as also implicitly assumed by Dukler and Hubbard and Nicholson et al.

The pressure drop along the stratified flow region, ΔP_{54}, can be computed from the differential momentum balances relative to the gas and the liquid layers

$$A_b\frac{dP}{dX}-\tau_i S_i-\tau_{wb}P_b-\rho_g g A_b\sin\theta=0, \quad (25)$$

$$\rho_l\frac{d}{dX}[(v_t-v_f)^2A_f]+A_f\frac{dP}{dX}+g\rho_l\cos\theta\frac{d}{dX}(A_f\xi)$$
$$-\tau_{wf}P_f+\tau_i S_i-A_f\rho_l g\sin\theta=0. \quad (26)$$

Equations 25 and 26 have been written with respect to the coordinate $X=v_t t-x$ (see Figure 1), assuming that the flow is stratified. In Eq. 25, the variations with X of gas momentum and height have been neglected.

The wall stresses τ_{wb} and τ_{wf} can be evaluated by

$$\tau_{wb}=\frac{1}{2}f_b\rho_g v_b^2,\quad \tau_{wf}=\frac{1}{2}f_f\rho_l v_f^2, \quad (27)$$

where the friction factors f_f and f_b are the same functions of the liquid and the gas Reynolds numbers and of the pipe roughness as in single-phase flow, with Re_{lf} and Re_{gb} defined as

$$Re_{lf}=\frac{4A_f}{P_g}\frac{v_f}{\nu_l},\quad Re_{gb}=\frac{4A_b}{P_b+S_i}\frac{v_b}{\nu_g}. \quad (28)$$

The shear stress at the gas-liquid interface, τ_i, can be expressed as

$$\tau_i=\frac{1}{2}f_i\rho_g(v_b-v_f)^2, \quad (29)$$

where the interfacial friction factor, f_i, can be evaluated by one of the equations recently proposed by Andreussi and Persen (1987) or Andritsos and Hanratty (1987). According to these equations, f_i is expressed as

$$f_i=\phi_i f_b, \quad (30)$$

where the coefficient ϕ_i is a function of main flow parameters.

Equations 25 and 26 can be integrated starting from the boundary condition at the bubble nose

$$X=0:\quad H_f=H_s,\quad v_f=v_s. \quad (31)$$

Equation 31 arises from the momentum balance at the bubble nose, Eq. 24, under conditions which are possibly verified when the bubble nose is centered (large Fr_m). This flow configuration is obviously different from the stratified configuration on which Eqs. 25 and 26 are based. Due to the gross approximations which lead to the formulation of Eqs. 25, 26 and 31 their integration is only meaningful for values of the mixture Froude number larger than a limiting value, Fr_{mc}, given by

$$Fr_{mc}=\sqrt{\cos\theta}\left(\frac{v_m}{v_t-v_m}\right)\sqrt{\frac{\pi}{4}\frac{H_s}{\sin\frac{\gamma}{2}}}. \quad (32)$$

where γ is the angle which subtends the liquid layer. This is because at $X=0$ the derivative dH_f/dX is positive for $Fr_m<Fr_{mc}$.

This critical Froude number has been related by Nicholson et al. to the minimum velocity necessary to prevent the gas bubble to penetrate into the slug under the effect of gravity. For $Fr_m<Fr_{mc}$, Nicholson et al. suggested to reduce the film holdup until the integration was possible. This corresponds to the use of the modified boundary condition

$$X=0:\quad v_f=\eta v_s, \quad (33)$$

with $\eta<1$ and H_f given by Eq. 3. Although it seems reasonable that $v_f(0)<v_s$, the physical explanation and the proposed solution to the problem given by Nicholson et al. do not appear to be satisfactory.

Considering the complex 3-D flow structure around the nose of the elongated gas bubble, it is difficult to propose a different solution to this problem, rather than limiting our attention to the case $Fr_m>Fr_{mc}$, with $\eta=1$. In this case, the integration of Eqs. 25 and 26 along the slug tail can proceed up to the point $X=l_f$, at which the gas and liquid mass balances are satisfied, giving as outputs of the integration the shape of tail, $H_f(X)$ and the pressure drop along the tail, ΔP_{54}.

Finally, the pressure drop through the slug unit can be computed by means of Eqs. 19, 20, 24 and 25, and after integration:

$$\Delta P_u=\rho_l H_s(v_t-v_s)[v_s-v_f(l_f)]+\rho_l g\cos\theta\left(\xi_1-\frac{D}{2}H_s\right)$$
$$+4\frac{l_s}{D}\tau_{ws}+\rho_m l_s g\sin\theta+\Delta P_{54}, \quad (34)$$

The frictional and gravitational pressure gradients can also be expressed as

$$-\left(\frac{dP}{dx}\right)_F=\frac{1}{l_u}\left\{4\frac{l_s}{D}\tau_{ws}+\frac{1}{A}\int_o^{l_f}(\tau_{wb}P_b+\tau_{wf}P_f)dX\right\}, \quad (35)$$

$$-\left(\frac{dP}{dx}\right)_G=[\rho_l H_l+\rho_g(1-H_l)]g\sin\theta. \quad (36)$$

As in Eq. 34, ΔP_{54} is often small when compared with the other terms, Eq. 34 can be more conveniently adopted rather than Eqs. 35 and 36 for the computation of the total pressure gradient.

Model equations so far considered can be made dimensionless adopting the pipe diameter as length scale and the liquid velocity as velocity scale. The pressure gradient can be normalized by means of the frictional pressure gradient relative to the liquid phase flowing alone in the pipe

$$\left(\frac{dP}{dx}\right)_l = 2f_l\rho_l j_l^2/D, \tag{37}$$

where the friction factor f_l is a function of the superficial liquid Reynolds number and, eventually, of the pipe roughness. Resulting equations depend on the dimensionless groups

$$\tilde{j}_g = \frac{j_g}{j_l}, \tag{38}$$

$$T = \frac{\rho_l j_l^2}{P}, \tag{39}$$

on the mixture Froude number, Fr_m, the density ratio, ρ_g/ρ_l, pipe inclination, θ, and on the gas and liquid superficial Reynolds numbers, Re_g and Re_l. The empirical closure relations used for ϕ_d, ϕ_i, v_t and H_s are expressed as functions of other dimensionless groups. These relations are reported in the Appendix. To solve model equations, it is also necessary to specify the slug frequency or the slug length. On the basis of a large set of experimental data, Nicholson et al. proposed that the ratio l_s/D could be assumed as about constant and equal to 30.

Outputs of the model are the dimensionless frictional pressure gradient

$$\Phi_F^2 = \frac{(dP/dx)_F}{(dP/dx)_l}, \tag{40}$$

The total (frictional, gravitational and acceleration) dimensionless pressure gradient, Φ_T^2

$$\Phi_T^2 = \frac{-dP/dx}{-(dP/dx)_l + \rho_l g \sin\theta} \tag{41}$$

the mean liquid holdup, given by Eq. 10, and the dimensionless slug frequency

$$\tilde{\nu}_s = \frac{v_t D}{j_l l_u}. \tag{42}$$

Long slug approximation

The solution of model equations is complicated by the integration of the gas and liquid momentum balances along the slug tail. This integration proceeds up to the position $X = l_f$ at which the liquid mass balance, Eq. 1, is satisfied. In order to simplify the computations, Dukler and Hubbard and Nicholson et al. assumed

$$\int_o^{l_f} v_f H_f dX \simeq v_f(l_f) H_f(l_f) l_f. \tag{43}$$

According to Eq. 43, the height and velocity of the liquid layer are constant and equal to the values obtained from the integration of the film momentum equation at $X = l_f$. This numerical approximation represents a significant structural change of the model. In fact, the differences between the two solutions are relevant, with the approximate solution being about 1.4 times the correct value for the full range of mixture velocities.

Model equations so far developed require as external input the slug length, and give as outputs the slug frequency and the ratio l_s/l_f, besides the pressure gradient and the mean liquid holdup. If the dimensionless slug length, l_s/D, is left as a free parameter, model equations can easily be solved in the two limiting cases: $l_s/D = 0$ (stratified flow), and $l_s/D \to \infty$ (Long Slud Model). In the LSM, as also the length of the stratified flow region increases with increasing l_s, it can be assumed that, in the limit $l_s/D \to \infty$, the height of the liquid film is constant and equal to the equilibrium value reached for $x/D \to \infty$. At the same time, the pressure drop due to the acceleration of the liquid film at the slug front becomes negligible when compared with frictional losses, as shown in Eq. 34.

The approximation introduced by Dukler and Hubbard and Nicholson et al. with Eq. 43 presents some similarities with the LSM. However, in that model the integration of the differential film momentum balance is still required, and film acceleration losses *are not neglected*. In the LSM, the differential equation describing film flow degenerates into an algebraic equation. At the same time, for $l_s/D \to \infty$, the slug frequency tends to zero and the LSM only gives as significant outputs the pressure gradient, the mean liquid holdup, identical to the value obtained with the general model, as shown in Eq. 13, and the ratio l_f/l_s. In the long slug approximation the slug frequency relative to a finite value of l_s/D can be computed as

$$\nu_s = \frac{v_t}{l_s(1 + l_f/l_s)}, \tag{44}$$

using for l_f/l_s the value obtained with the LSM.

The effect of slug length on the dimensionless pressure gradient, Φ_F^2, is shown in Figure 2. Quite interestingly, Figure 2 indicates that the effects of l_s/D on Φ_F^2 are fairly small, the maximum difference between the cases $l_s/D = 15$ and $l_s/D \to \infty$ being 15% for large values of $\tilde{j}_g$. This can be explained considering that, at increasing l_s/D, the relative magnitude of frictional losses with respect to film acceleration losses increases, while the ratio l_f/l_s decreases. These two effects compensate each other almost exactly.

Figure 3 indicates a strong effect of l_s/D on $\tilde{\nu}_s$. In this figure, the theoretical predictions are compared with a set of data reported by Nydal (1991) and obtained in this laboratory under the same conditions as present experiments. In these measurements, l_s/D was in all cases close to 15. From Figure 3 it can easily be seen that the LSM is largely in error in the prediction of both the absolute value of $\tilde{\nu}_s$, computed by means of Eq. 44 with $l_s = 15D$, and its trend at increasing $\tilde{j}_g$. It follows that when the slug length is known, the slug frequency should be computed with the complete model presented in this article.

In practical applications, such as the design of gas-liquid transportation lines, the information required about slug flow are essentially the pressure gradient and the mean liquid holdup. Other information, such as the slug frequency, or the maximum

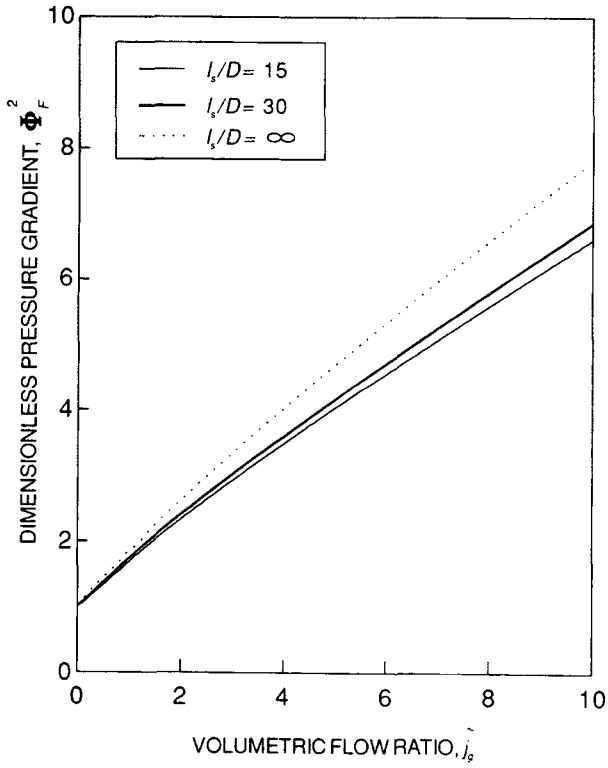

Figure 2. Effects of l_s/D on Φ_F^2.

$Fr_l = 1.4$, $T = 0$, $\rho_g/\rho_l = 1.2\ 10^{-3}$, $\theta = 0$, $Re_l = 5\ 10^4$, $Bo = 330$.

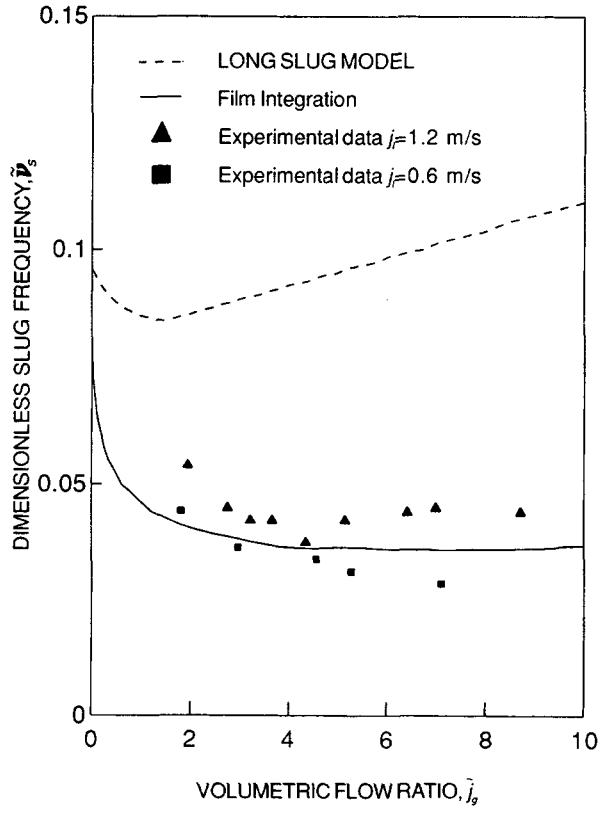

Figure 3. Comparison between experimental and computed values of the dimensionless frequency.

$Fr_l = 1.4$, $T = 0$, $\rho_g/\rho_l = 1.2\ 10^{-3}$, $\theta = 0$, $Re_l = 5\ 10^4$, $Bo = 330$.

slug length, are also needed, but there is evidence that available predictive methods for these parameters fail when applied to long pipelines. In particular, it has been reported in a number of technical articles (see, for instance, Scott et al., 1987) that the slug length steadily increases in long pipelines with variable slope. It is then concluded that the LSM can be a very useful design tool, able to give the same information as more complex models in a much shorter computational time.

Although model equations apparently depend on a large number of dimensionless parameters, the sensitivity of the LSM to many of these parameters (such as Re_l, Re_g, Fr_m, ϕ_i, ρ_g/ρ_l and so on) is low and Φ_F^2 and H_l are essentially functions of $\tilde{j}_g$ and θ. These functions, computed for $\theta = 0$, are compared in Figure 4 with the model presented by Nicholson et al. and with the empirical correlation proposed by Lockhart and Martinelli (1949). Considering the boundaries of the slug-flow regime, and that most of the available data are relative to $\tilde{j}_g < 10$, the three models compared in Figure 4 give quite similar results. Nicholson et al. and recently Stanislav et al. (1986) have compared their model with a large set of data. A simple inspection of these data and the comparison reported in Figure 4 indicates that the LSM gives a similarly good fit to these measurements. In the second part of this article, the LSM and the Nicholson et al. model will be compared with a new set of measurements obtained in this laboratory under different experimental conditions than previously published data.

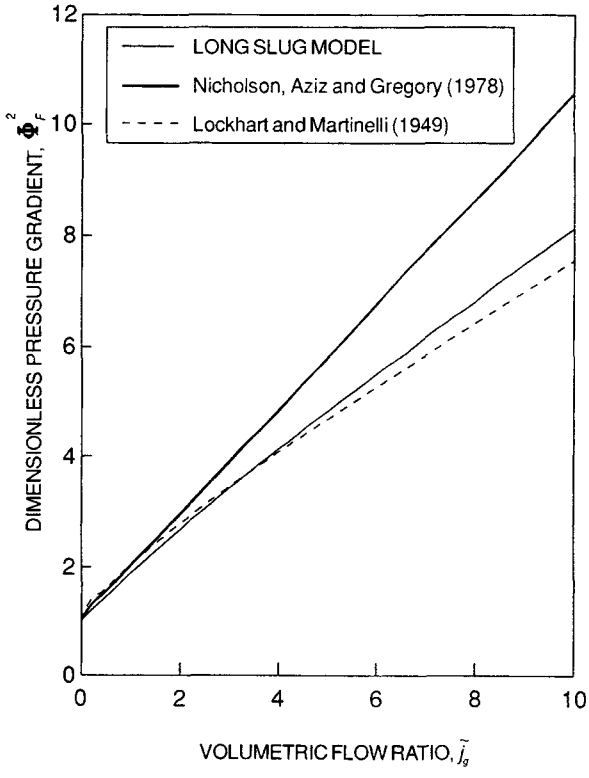

Figure 4. Comparison between the dimensionless pressure gradient Φ_F^2 computed as proposed by Lockhart and Martinelli (1949), Nicholson et al. and in this article.

$Fr_l = 1.4$, $T = 0$, $\rho_g/\rho_l = 1.2\ 10^{-3}$, $\theta = 0$, $Re_l = 5\ 10^4$, $Bo = 330$.

Apparatus

The apparatus includes an inclinable bench, 17 m long, the slope of which can be varied continuously in the range ±3° by means of a motorized support. The test section consists of transparent Plexiglass tubes with inner diameters of 18, 50, and 90 mm and maximum length equal to the length of the bench. The tubes are made of carefully flanged, 2 m long interchangeable sections mounted on the bench by precision supports. A stainless steel tube 53 mm ID has also been used in the experiments. In order to test the effect of pipe length, two pipes of the same diameter (50 mm) were mounted on the bench and connected at one end with a long radius (1 m) circular bend which reversed the flow from one pipe to the other.

The liquid, water in present experiments, is circulated by two centrifugal pumps of different capacity. Air is supplied from a high-pressure line. Air and water are metered by two sets of rotameters. The air outlet pressure was in all cases close to atmospheric conditions. Liquid and gas are fed to the pipe through a Tee section. At liquid entrance, stratified flow conditions are created by a thin diaphragm which separates liquid inlet (from below) from gas inlet (along flow direction).

The void fraction has been measured by a conductance probe made of two ring electrodes mounted flush to the pipe wall. A detailed description of the behavior of this probe is reported by Andreussi et al. (1988). The absolute pressure and the pressure drop between two pressure taps spaced 2 m apart have been measured by two piezoresistive absolute transducers and by one inductive differential transducer.

Most of the measurements of the differential pressure have been taken between pressure taps located at 7.0 and 5.0 m from the gas-liquid separator (kept at atmospheric pressure). A number of tests have been made in order to check the presence of exit effects on the experimental readings. In these tests, the distance of the measuring section from the separator was varied in the range 2-9 m, but no appreciable changes have been noticed.

Experimental Results and Discussion

In the research project described in this article, about 250 experimental measurements have been obtained. These data cover three pipe diameters (18, 50, 90 mm), 4 inclinations (0°, ±3°, .3°), two pipe lengths (17 and 34 m). As shown in Figure 5, where data points are reported on the Mandhane (1974) flow chart, present measurements cover the slug flow region and extend significantly into the dispersed and elongated bubble flow patterns.

The effect of pipe length on pressure drop has only been checked for horizontal flow. In Figure 6 data taken under identical conditions except for the pipe length are compared. It can be noticed that the two sets of data are almost indistinguishable, thus removing the possible objection that a pipe length of 17 m is not sufficient to obtain developed flow conditions.

The effect of a downward pipe inclination on pressure losses is considered in Figure 7. As can be seen, the experimental measurements do not agree with theory (lower line) in the range of low $\tilde{j}_g$. In the empirical methods developed for predicting pressure losses in long pipelines (see, for instance, Baker and Gravestock, 1987), it is common practice to neglect the gravitational pressure recovery in downhill sections of the pipeline. When this is done with present measurements (upper line in Figure 7) the agreement between theory and experiments greatly improves.

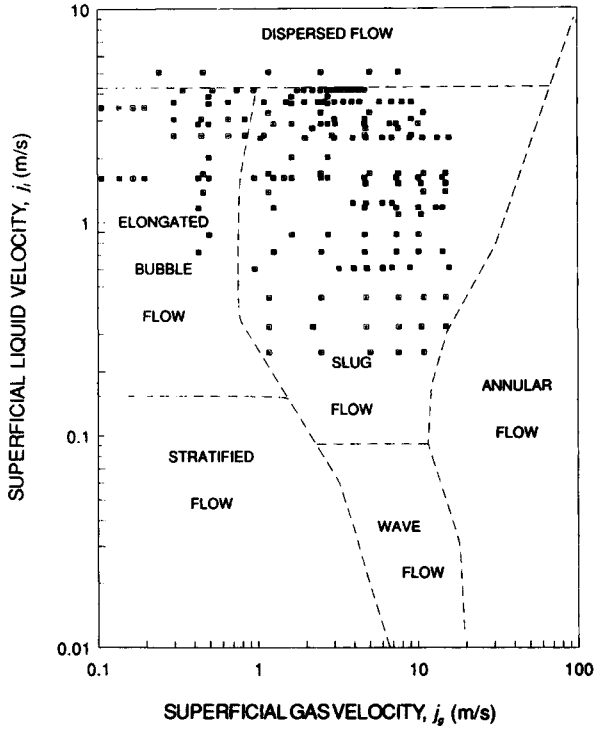

Figure 5. Mandhane flow pattern map and experimental data.

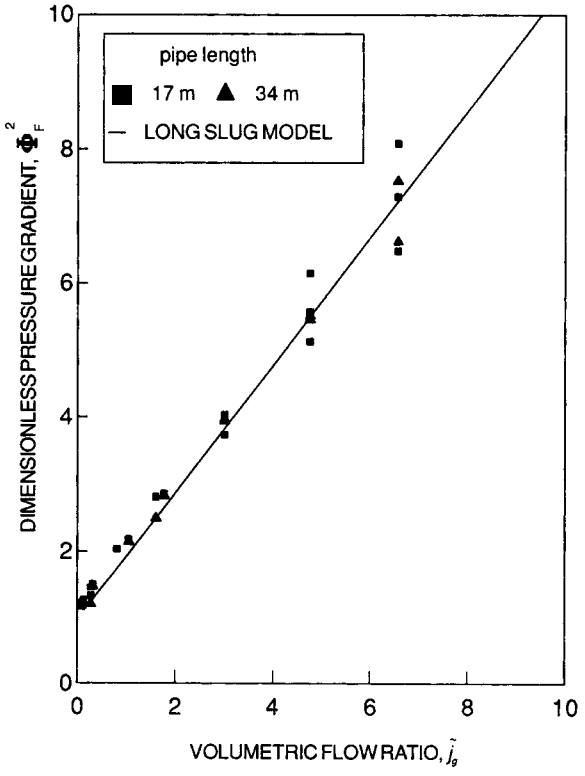

Figure 6. Effect of pipe length on the experimental measurements of the pressure gradient.

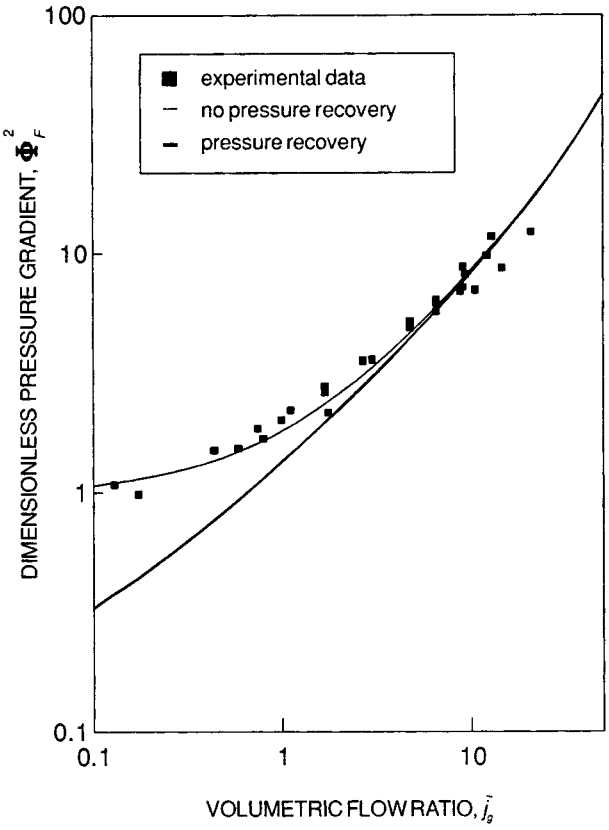

Figure 7. Comparison between theory and experiments relative to a downward inclination ($\theta = -3.0°$).

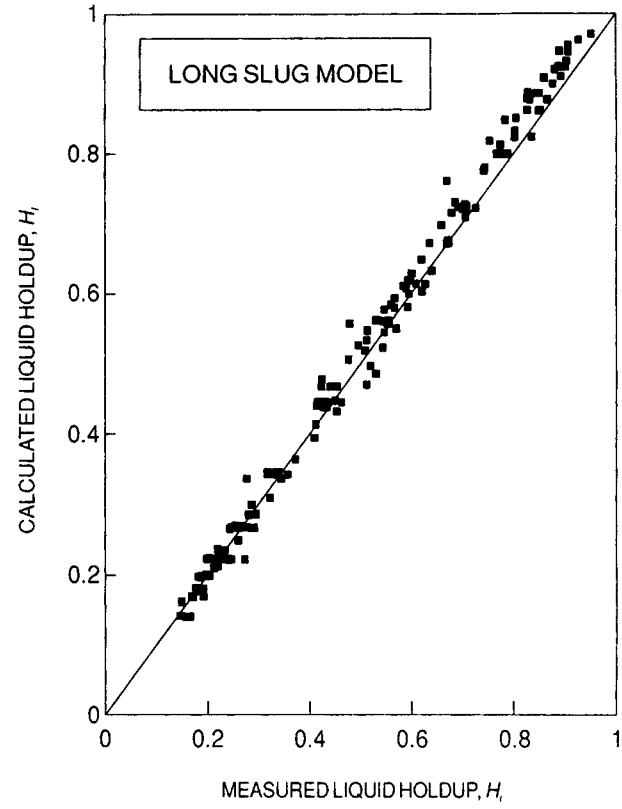

Figure 8. Comparison between computed and experimental values of the liquid holdup.

As shown in Figures 8 and 9, all the experimental measurements are very well predicted by the present theory, with an error mean square of less than 6% for the mean liquid holdup and less than 10% for the pressure gradient. It should be remarked that data relative to very different flow conditions and geometry are equally well fitted by the LSM. In particular, it is important to notice that the data considered in Figures 8 and 9 significantly extend into the dispersed and elongated bubble flow patterns and that the LSM gives an adequate fit to all these data. Elongated bubble flow is structurally similar to slug flow and it is not surprising that the same model can be used for the two regimes. Dispersed bubble flow is usually considered as a distinct flow pattern. However, it can be noticed that slug, elongated and dispersed bubble flow can all be described as flow regimes in which the gas phase presents various degrees of dispersion in a continuous liquid phase. Experimental and computed values of the dimensionless pressure gradient relative to a liquid flow rate at which both dispersed bubble and slug flow are observed at increasing gas flow, are plotted vs. $\tilde{j}_g$ in Figure 10. As can be seen, the transition between these flow patterns is smooth, and the model gives a very good fit to all these measurements.

A close examination of the data represented in Figure 9 reveals that in many cases the LSM slightly underpredicts the measured pressure gradient. In Figure 2, it is shown that the pressure gradient computed for $l_s/D \to \infty$ is up to 15% greater than the case $l_s/D \simeq 15$–20, and if we use the complete model to compute the pressure gradient, the differences between measured and computed values of the pressure gradient are of

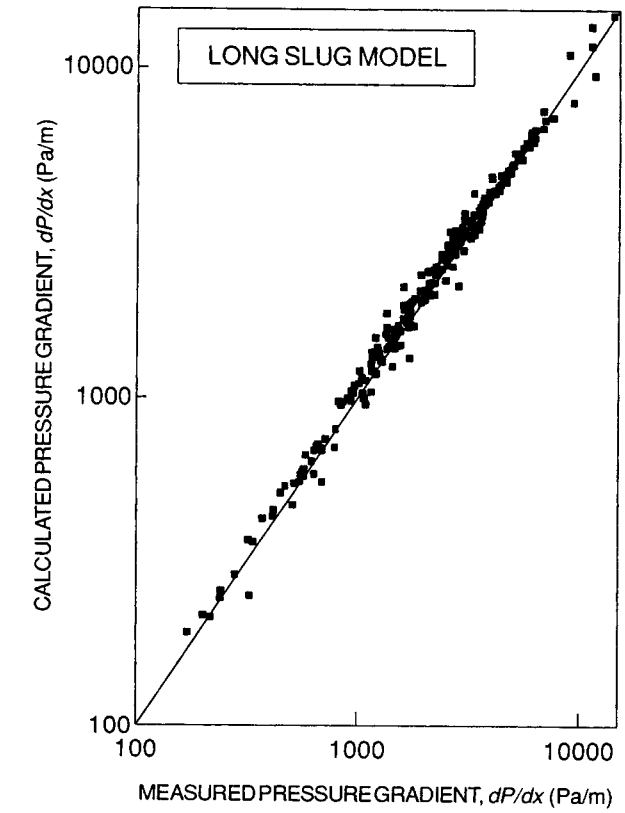

Figure 9. Comparison between computed and experimental values of the pressure gradient.

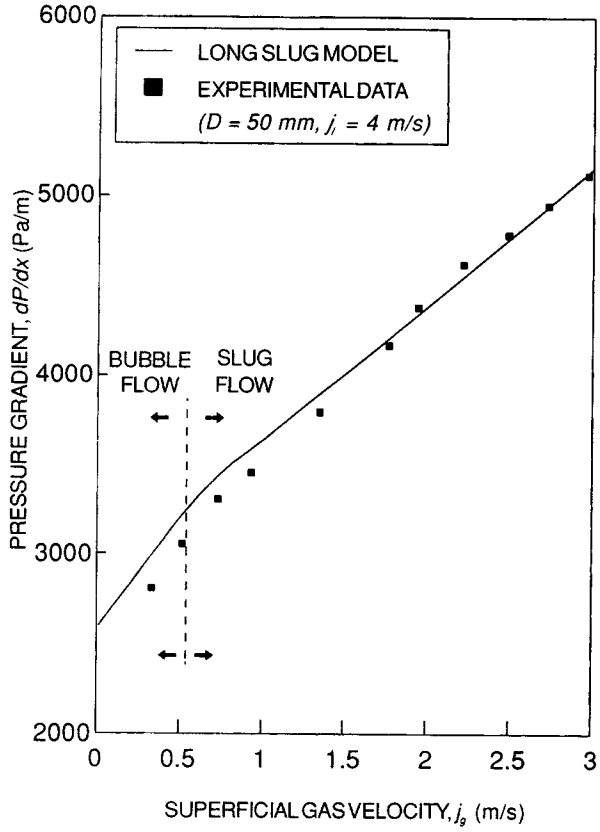

Figure 10. Comparison between computed and experimental values of the pressure gradient at the transition between bubble and slug flow.

$j_l = 4.0$ m/s, $\theta = 0°$.

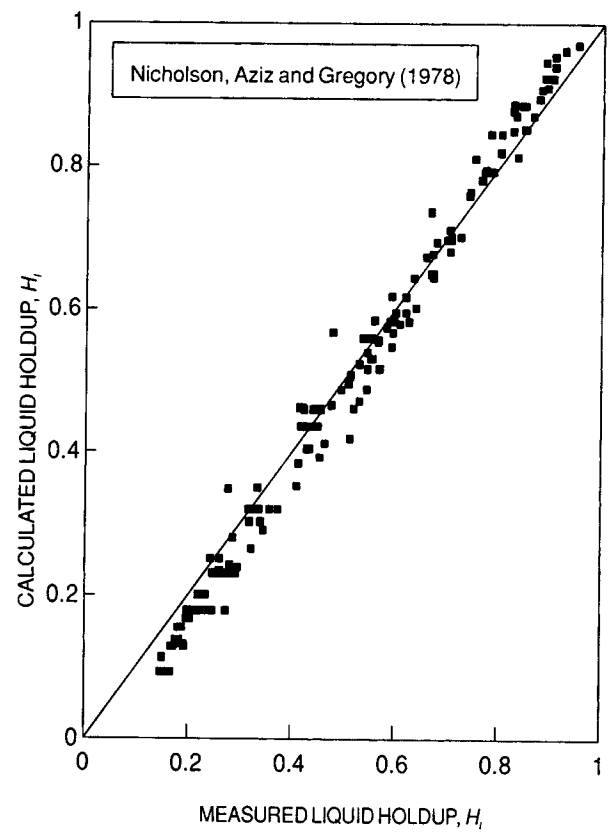

Figure 11. Comparison of present measurements of the liquid holdup with the model proposed by Nicholson et al.

the order of 15-20%. This should not be surprising if it considered that both versions of the model are based on a fairly approximate representation of slug flow and do not contain adjustable parameters.

In particular, as reported by Nydal et al. (1992), even in fairly long pipes there is evidence of phenomena such as the formation of new slugs, their growth, coalescence and, eventually, decay. All these phenomena will contribute to an increase of pressure losses with respect to the idealized case on which the present flow model is based.

Present data are compared in Figures 11 and 12 with the model of slug flow proposed by Nicholson et al. As can be noticed from these figures, this model also gives an acceptable overall fit to the experimental measurements. The larger scatter and some systematic errors in the prediction of the mean liquid holdup should be attributed to the different correlation adopted by Nicholson et al. to predict void in the slugs. This correlation is only based on data relative to air-light oil mixtures and, as shown by Andreussi and Bendiksen (1988), it does not give an acceptable fit to data relative to different fluid pairs.

Pressure gradient measurements show a larger scatter when compared with the Nicholson et al. model rather than with the LSM (Error Mean Square = 0.16 for Nicholson et al. and 0.10 for the LSM). A careful analysis of data reveals that the Nicholson et al. model is increasingly in error when the bubble flow regime is approached (large j_l). This is due to the fact that in this model the frictional pressure gradient is given by the sum of two terms: *frictional losses* in the slug body, simply computed assuming homogeneous flow, and *film acceleration losses*. The homogeneous flow approximation causes an appreciable error in the computation of frictional losses relative to the slug body, when void in the slugs becomes large. This error is compensated by the approximation introduced with the use of Eq. 43. When bubble flow is approached, film acceleration losses tend to zero and the pressure gradient is only related to frictional losses, which in the Nicholson et al. model are underpredicted.

Conclusions

A mechanistic model of slug flow based on the original work of Dukler and Hubbard (1975) and on a set of empirical closure relations has been presented. A simplified version of the model, which physically corresponds to the flow of long liquid slugs (LSM), immediately arises from the general model. It is shown that the LSM gives almost identical results as the more general model, when the comparison is limited to the prediction of the pressure gradient and the mean liquid holdup. When the mean slug length is known, the slug frequency can be predicted with good accuracy by means of the general model, while the LSM is largely in error.

The LSM combines the dispersed bubble and the stratified flow patterns through the use of gas and liquid continuity equations and of closure relations for the slug translational velocity and for the void in the slugs. These closure relations

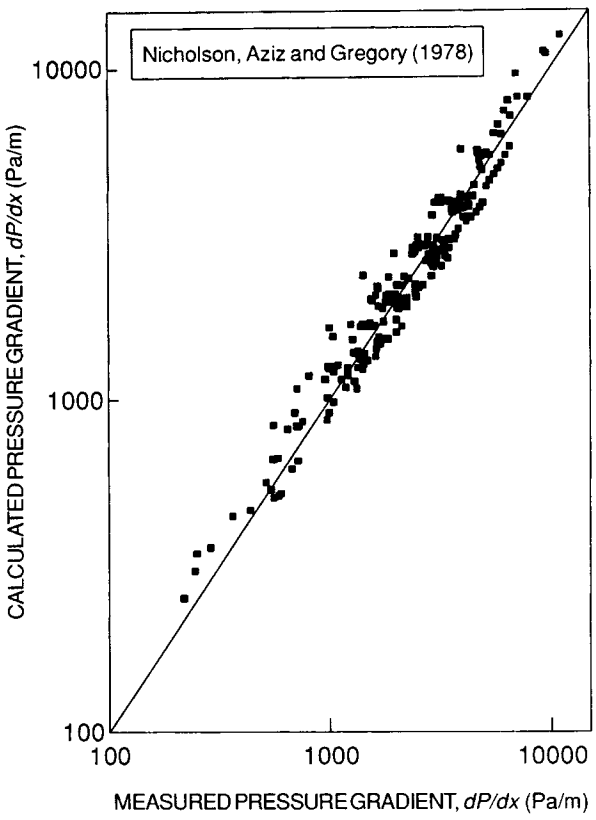

Figure 12. Comparison of present measurements of the pressure gradient with the model proposed by Nicholson et al.

and, as well, the friction factors introduced in order to predict the pressure gradient have been derived from the literature. When new, better founded correlations will be available for these parameters, the model could be easily updated. It should also be remarked that *the model does not contain adjustable parameters*. Due to its simple structure, the model appears to be suitable for extensive use in the design and analysis of long pipelines transporting gas-liquid mixtures.

The LSM gives a very good fit to a set of experimental data produced in this laboratory and relative to three pipe diameters, four inclinations and two lengths. These data cover the slug, elongated, and dispersed bubble flow patterns. The results of the present investigation suggest that a unique predictive model can be used to describe all these flow patterns and, in the limit $l_s/l_f \to 0$, stratified flow, also.

Acknowledgments

This work has been supported by the Commission of the European Communities under Contract EN3G-0047/I.

Notation

A = cross section
Bo = Bond number, see Eq. A9
c_o = constant in Eq. 5
D = pipe diameter
f = friction factor
F = dimensionless number, see Eq. A12
Fr_l = Froude number based on the liquid superficial velocity
Fr_m = Froude number based on mixture velocity, see Eq. 7
Fr_{mc} = critical Froude number, see Eq. 32
F_o, F_1 = constants in Eq. 6
g = acceleration of gravity
H = liquid holdup
j = superficial velocity
l = length
P = pressure
P_b, P_f = perimeter wetted by gas, liquid in stratified flow
Re = Reynolds number
S_i = length of interfacial chord
t = time
T = dimensionless parameter, see Eq. 39
v = velocity
v_o = constant velocity in Eq. 5, see Appendix
v_∞ = terminal velocity of a bubble in a stationary liquid, see Eq. A14
x = axial coordinate
X = $v_l t - x$

Greek letters

γ = angle which subtends the liquid film in stratified flow
θ = pipe inclination with respect to the horizontal
ν = kinematic viscosity
ν_s = slug frequency
ρ = density
σ = interfacial tension
τ = shear stress
ξ = depth of the center of pressure
ϕ = friction factor multiplier
Φ_F = dimensionless frictional pressure gradient
Φ_T = dimensionless total pressure gradient

Subscripts and superscripts

A = acceleration
b = elongated gas bubble
d = dispersed bubble flow
f = liquid film
F = frictional
g = gas phase
G = gravitational
i = gas-liquid interface
l = liquid phase
m = gas-liquid mixture
s = slug
t = translational
u = slug unit
w = pipe wall
$\tilde{\ }$ = dimensionless parameter
$\bar{\ }$ = mean value

Literature Cited

Andreussi, P., and L. N. Persen, "Stratified Gas-Liquid Flow in Downwardly Inclined Pipes," *Int. J. Multiphase Flow*, **13**, 565 (1987).

Andreussi, P., A. Di Donfrancesco, and M. Messia, "An Impedance Method for the Measurement of Liquid Holdup in Two-Phase Flow," *Int. J. Multiphase Flow*, **14**, 777 (1988).

Andreussi, P., and K. Bendiksen, "An Investigation of Void Fraction in Liquid Slugs for Horizontal and Inclined Gas-Liquid Pipe Flow," *Int. J. Multiphase Flow*, **15**, 937 (1989).

Andritsos, N., and T. J. Hanratty, "Influence of Interfacial Waves in Stratified Gas-Liquid Flows," *AIChE J.*, **33**, 444 (1987).

Baker, A. C., and N. Gravestock, "New Correlations for Predicting Pressure Loss and Holdup in Gas/Condensate Pipelines," *3rd International Conference on Multiphase Flow*, The Hague, Netherlands (1987).

Bendiksen, K., "An Experimental Investigation of the Motion of Long Bubbles in Inclined Tubes," *Int. J. Multiphase Flow*, **10**, 467 (1984).

Dukler, A. E., and M. G. Hubbard, "A Model for Gas-Liquid Slug

Flow in Horizontal Tubes," *Ind. Eng. Chem. Fundam.*, **14**, 337 (1975).
Fabre, J., G. Ferschneider, and L. Masbernat, "Intermittent Gas Liquid Flow Modelling in Horizontal or Weakly Inclined Pipes," *Int. Conf. on Physical Modelling of Multiphase Flow*, Coventry, U.K. (1983).
Lockhart, R. W., and R. C. Martinelli, "Proposed Correlation of Data for Isothermal Two-Phase, Two-Components Flow in Pipes," *Chem. Eng. Prog.*, **45**, 39 (1949).
Malnes, D., "Slug Flow in Vertical, Horizontal and Inclined Pipes," IFE/KR/E-83/002 Institute for Energy Technology, Kjeller, Norway (1983).
Mandhane, J. M., G. A. Gregory, and K. Aziz, "A Flow Pattern Map for Gas-Liquid Flow in Horizontal Pipes," *Int. J. Multiphase Flow*, **1**, 537 (1974).
Marie, J. L., "Modelling of the Skin Friction and Heat Transfer in Turbulent Two-Component Bubbly Flows in Pipes," *Int. J. Multiphase Flow*, **13**, 309 (1987).
Nicholson, M. K., K. Aziz, and G. A. Gregory, "Intermittent Two-Phase Flow in Horizontal Pipes: Predictive Models," *Can. J. Chem. Eng.*, **56**, 653 (1978).
Nicklin, D. J., J. O. Wilkes, and J. F. Davidson, "Two-Phase Flow in Vertical Tubes," *Trans. Inst. Chem. Engs.*, **40**, 61 (1962).
Nydal, O. J., "An Experimental Investigation of Slug Flow," PhD Thesis, University of Oslo (1991).
Nydal, O. J., S. Pintus, and P. Andreussi, "Statistical Characterization of Slug Flow," *Int. J. Multiphase Flow*, **18**, 439 (1992).
Scott, S. L., O. Shoham, and J. Brill, "Modelling Slug Growth in Large Diameter Pipes," *Int. Conf. Multi-Phase Flow*, The Hague, Netherlands (1987).
Stanislav, J. F., S. Kokal, and M. K. Nicholson, "Gas-Liquid Flow in Downward and Upward Inclined Pipes," *Can. J. Chem. Eng.*, **64**, 881 (1986).

Appendix

Slug translational velocity

According to Bendiksen (1984), the values of c_o and v_o in Eq. 5 depend on the mixture Froude number, Fr_m, defined in Eq. 7. Bendiksen proposed:

$Fr_m \le 3.5$:

$$c_o = 1.05 + 0.15 \text{ sen}^2\,\theta, \tag{A1}$$

$$v_o = (0.351 \sin\theta + 0.542 \cos\theta)\sqrt{gD}; \tag{A2}$$

$Fr_m > 3.5$:

$$c_o = 1.2, \tag{A3}$$

$$v_o = 0.351 \sin\theta\sqrt{gD}. \tag{A4}$$

These values hold for upward and horizontal flows. Downward flow is more complicated, as at low mixture velocities the elongated bubble velocity can eventually be negative. The model of slug flow presented in this article holds for large values of Fr_m, as shown in Eq. 32, and the definition of slug flow given in the Introduction requires the slug body to the aerated, or $Fr_m > F_o$ in Eq. 6. Therefore, the behavior of elongated bubbles at low velocities is not considered and the above equations are extended to downward flow as follows: Eq. A1 is modified into

$$c_o = 1.0 + 0.2 \sin^2\theta. \tag{A5}$$

Equation A4 only holds for $\theta \ge 0$, for $\theta < 0$ it is assumed

$$v_o = 0. \tag{A6}$$

Equations A5 and A6 give a better overall prediction of the experimental results reported by Bendiksen (1984). Unfortunately in downward flow these experiments are limited to low inclinations (up to 30°) and fairly low mixture velocities.

Void in the slugs

In the correlation proposed by Andreussi and Bendiksen (1989), Eq. 6, F_o and F_1 are given by the empirical equations

$$F_o = 2.6\left(1 - 2\frac{D_o^2}{D^2}\right), \tag{A7}$$

$$F_1 = 2{,}400\left(1 - \frac{\sin\theta}{3}\right)Bo^{-3/4}, \tag{A8}$$

where $D_o = 2.5$ cm and Bo is the Bond number defined as

$$Bo = \frac{(\rho_l - \rho_g)gD^2}{\sigma}. \tag{A9}$$

Equation A7 holds for $D \ge \sqrt{2}D_o$; for $D < \sqrt{2}D_o$, $F_o = 0$.

Interfacial friction factor

The correlation proposed by Andreussi and Persen (1987) can be restated as

$F \le 0.36$:

$$\phi_i = 1.0, \tag{A10}$$

$F > 0.36$:

$$\phi_i = 1.0 + 29.7(F - 0.36)^{0.67}\left(\frac{h_l}{D}\right)^{0.2}, \tag{A11}$$

where the dimensionless number F is defined as

$$F = \left(\frac{\rho_g}{\rho_l - \rho_g}\frac{S_i}{A_b}\frac{1}{g\cos\theta}\right)^{1/2}(v_b - v_f). \tag{A12}$$

This correlation is only based on data taken at low downward inclinations.

Friction factor in bubbly flow

According to the definitions given in the text, as shown in Eq. 22, the coefficient ϕ_d can be related to the friction factor multiplier used by Malnes (1983) by the equation

$$\phi_d = \frac{1}{H_s}\left[1 + 15.3\frac{(1 - H_s)}{\sqrt{H_s}}\frac{v_\infty}{v_m}\right]. \tag{A13}$$

where v_∞ is the terminal velocity of an isolated bubble rising in an infinite medium, given by

$$v_\infty = 1.18\left[\frac{g\sigma(\rho_l - \rho_g)}{\rho_l^2}\right]^{0.25}. \tag{A14}$$

Manuscript received Apr. 16, 1991, and revision received Aug. 4, 1992.